Journal of ELECTRONIC MATERIALS, Vol. 36, No. 10, 2007
DOI: 10.1007/s11664-007-0203-8

Regular Issue Paper

Neutron Radiation Effects in Epitaxially Laterally Overgrown GaN Films

A.Y. POLYAKOV,[1] N.B. SMIRNOV,[1] A.V. GOVORKOV,[1] A.V. MARKOV,[1] E.B. YAKIMOV,[2] P.S. VERGELES,[2] N.G. KOLIN,[3] D.I. MERKURISOV,[3] V.M. BOIKO,[3] IN-HWAN LEE,[4] CHEUL-RO LEE,[4] and S.J. PEARTON[5,6]

1.—Institute of Rare Metals, B. Tolmachevsky 5, Moscow 119017, Russia. 2.—Institute of Microelectronics Technology RAS, Chernogolovka 142432, Russia. 3.—Obninsk Branch of Federal State Unitary Enterprise, Karpov Institute of Physical Chemistry, Kiev Avenue, Obninsk Kaluga Region 249033, Russia. 4.—School of Advanced Materials Engineering and Research Center for Advanced Materials Development, Engineering College, Chonbuk National University, Chonju 561-756, Korea. 5.—Department of Materials Science Engineering, University of Florida, Gainesville Florida 32611, USA. 6.—e-mail: spear@mse.ufl.edu

Neutron radiation effects were studied in undoped *n*-GaN films grown by epitaxial lateral overgrowth (ELOG). The irradiation leads to carrier removal and introduces deep electron traps with activation energy 0.8 eV and 1 eV. After the application of doses exceeding 10^{17} cm^{-2}, the material becomes semi-insulating *n*-type, with the Fermi level pinned near the level of the deeper electron trap. These features are similar to those previously observed for neutron irradiated undoped *n*-GaN prepared by standard metal–organic chemical vapor deposition (MOCVD). However, the average carrier removal rate and the deep center introduction rate in ELOG samples is about five-times lower than in MOCVD samples. Studies of electron beam induced current (EBIC) show that the changes in the concentration of charged centers are a minimum in the low-dislocation-density laterally overgrown regions and radiation-induced damage propagates inside these laterally overgrown areas from their boundary with the high-dislocation-density GaN in the windows of the ELOG mask.

Key words: GaN, ELOG, neutron irradiation

INTRODUCTION

GaN and related InGaAlN solid solutions are important wide-bandgap semiconductors with multiple applications in UV/visible injection lasers and light-emitting diodes, high-frequency field effect transistors, and solar-blind photodetectors.[1,2] One problem is the lack of a lattice matched substrate, which makes it necessary for nitride films to be grown on sapphire or SiC. As a result, even when the low-temperature GaN or AlN buffers techniques are employed, the GaN epitaxial layers contain dislocation densities of ~10^9 cm^{-2}.[1] High dislocation densities adversely affect the lifetime of injection lasers and are reduced by the epitaxial lateral overgrowth (ELOG) technique.[1,3,4] In the most popular version of this technique a GaN template is grown by metal–organic chemical vapor deposition (MOCVD). Then, a mask of SiO_2 stripes is prepared by lithography, and a thick GaN layer is grown over the masked surface. The material above the mask grows predominantly in the lateral direction and has a dislocation density from two to three orders of magnitude lower than the material grown in the windows of the SiO_2 mask, for which the dislocation density is the same as for standard MOCVD layers. GaN films with local dislocation density ~10^6 cm^{-2} have been demonstrated and proved instrumental in realizing long-lived GaN-based injection lasers operating in continuous wave mode.[2]

It is of interest for one to understand how ionizing radiation will affect the properties of such material

(Received April 24, 2007; accepted June 25, 2007; published online August 15, 2007)

and how the radiation hardness of ELOG GaN compares with the radiation hardness of standard GaN. The main issues are the difference in the dislocation density, doping, and electrical and structural uniformity of these two types of materials. Radiation effects for the high-dislocation-density *n*-GaN films have been reported for electron, proton, neutron, and heavy ions irradiation.[4–13] For electron irradiation, the dominant radiation defects are shallow electron traps with activation energies 0.13, 0.16, and 0.18 eV that were attributed to nitrogen vacancies or their complexes.[5–7] For heavier particles, or for high electron doses, deeper electron traps with levels near E_c –0.8 eV and E_c –(1–1.2) eV were dominant.[8–10,12] The former was associated with Ga-interstitial-related centers, and the latter with N-interstitial-related defects.[8,12] Neutron irradiation was shown to produce mainly disordered regions whose core was comprised predominantly of the 0.8 eV and 1 eV interstitials-related defects.[10] After irradiation with high doses of fast neutrons, the Fermi level was pinned between the levels of these defects.[11]

For ELOG samples, the data for radiation effects are rather fragmentary. Proton irradiation with energy of 1.8 MeV leads to a heavy compensation of the material and introduces hole traps with an activation energy of 0.2 eV.[12] For high neutron doses of ELOG samples, the Fermi level is pinned at approximately the same position as in standard samples.[11] Preliminary results suggest that the types of deep centers created by neutrons in ELOG *n*-GaN are similar to the ones observed for high-dislocation-density MOCVD material, but the average carrier removal rate and the average deep defects introduction rates are lower for ELOG.[14]

Concerns in the study of radiation effects in ELOG material include the non-uniformity of structuralproperties (the existence of the high-dislocation-density and the low-dislocation density regions within one sample) and electrical and recombination properties (the doping level for the material grown in the windows of the SiO_2 mask is several times higher than in the ELOG region, while the diffusion lengths in the former areas are lower). In this paper we present studies of the electrical properties, diffusion lengths and deep trap spectra of neutron irradiated *n*-GaN in which we took such non-uniformities into account.

EXPERIMENTAL

ELOG films were grown on (0001) sapphire substrates using low temperature GaN buffers. First, 2 μm thick, undoped GaN layers were grown by standard MOCVD. Then, a pattern of 12 μm wide SiO_2 stripes, with 4-μm-wide gaps between the stripes, was deposited on MOCVD GaN templates, and 12 μm thick, undoped GaN epilayers were prepared by ELOG. Characterization involved capacitance–voltage (*C–V*) profiling, deep level transient spectroscopy (DLTS) with electrical and optical injection (the latter for hole traps spectra measurements; for brevity this technique will be called ODLTS), electron beam induced current (EBIC) profiling and mapping, and measurements of the EBIC signal collection efficiency dependence on the accelerating voltage of the probing electron beam. The latter technique allows one to estimate local values of minority carrier diffusion length and the local concentrations of the charged centers that determine the width of the space charge region.[15–19] In was used for ohmic contacts, and Schottky contacts were prepared by vacuum evaporation of Au through a shadow mask. The electrical properties of the ELOG films have been reported previously.[20–22] For deep trap parameters in heavily compensated irradiated samples we used photo-induced current transient spectroscopy (PICTS).[23,24] Fast reactor neutron irradiation was performed in a WWR-c type reactor with doses of 10^{13} to 10^{18} cm^{-2} neutrons. Thermal neutrons in these experiments were filtered out by Cd foil; the temperature of the samples during irradiation did not exceed 30°C.

RESULTS

Results of *C–V* Profiling and Admittance Spectroscopy

A typical concentration profile deduced from *C–V* measurements on virgin ELOG samples is presented in Fig. 1 (solid line). The net donor concentration is highly non-uniform. The concentration shows a plateau at ~3×10^{14} cm^{-3} for thicknesses of 1.3–1.8 μm, increasing to about 10^{15} cm^{-3} towards the surface and to ~3×10^{15} cm^{-3} deeper than 2 μm inside the diode. Irradiation with low neutron doses of 4×10^{13} cm^{-2} and 9×10^{13} cm^{-2} changed the concentration in the plateau region slightly, as shown in Fig. 2. After irradiation with 10^{15} cm^{-3}, the entire first 3 μm of the sample was fully depleted, while the concentration in the deeper region was lower than before irradiation (dashed

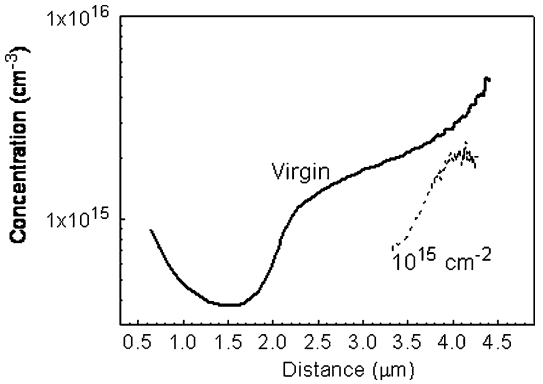

Fig. 1. Concentration profiles deduced from 300 K *C–V* measurements for ELOG *n*-GaN. Solid curve represents the virgin sample; the dashed curve represents the sample irradiated with 10^{15} cm^{-2} neutrons.

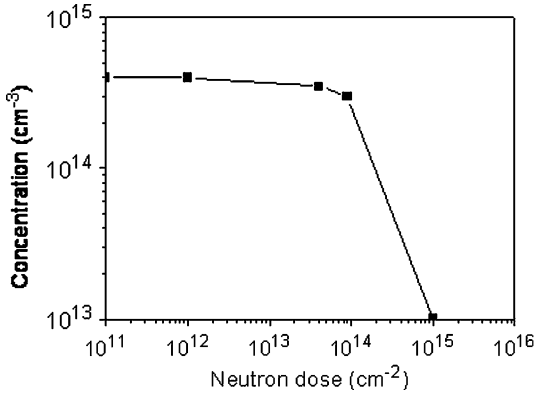

Fig. 2. Changes in electron concentration induced by neutron irradiation of ELOG *n*-GaN with small doses of neutrons; the values were obtained from *C–V* profiling and correspond to the low-concentration plateau in Fig. 1.

curve in Fig. 1). A higher dose of 2×10^{15} cm^{-2} resulted in the capacitance at 300 K being a fixed value of 12 pF for all studied frequencies (10 Hz to 10 MHz) and independent of applied voltage, as expected for a dielectric layer 5 μm thick. At higher temperatures, capacitance increased and showed a step, while the AC conductance G showed a peak (Fig. 3; the conductance shown in the figure is divided by the circular frequency so that the peak heights are equalized at various frequencies).[25] The temperature corresponding to the middle of the step in $C(T)$ or to the peak position in G/ω (T) dependancies shifted to higher values with increased frequency. Standard admittance spectroscopy analysis yielded, for the activation energy, 0.8–0.9 eV.[25] The $1/C^2$ versus voltage plots from 400 K low frequency *C–V* measurements were linear, and the concentration calculated from the slope was 4×10^{15} cm^{-3}. These results suggest the formation of a highly resistive layer in which the Fermi level is pinned near E_c –(0.8–0.9) eV and the concentration of uncompensated Fermi level pinning centers is ~10^{15} cm^{-3}. A further increase in dose to 6×10^{15} cm^{-2} increased the concentration of the deep 0.8–0.9 eV traps, pinning the Fermi level to 2.4×10^{16} cm^{-3}. For higher doses (2×10^{17} cm^{-2} and 10^{18} cm^{-2}), the entire volume of the samples became the highly resistive *n*-type, with the Fermi level pinned near E_c –0.95 eV.[10,11]

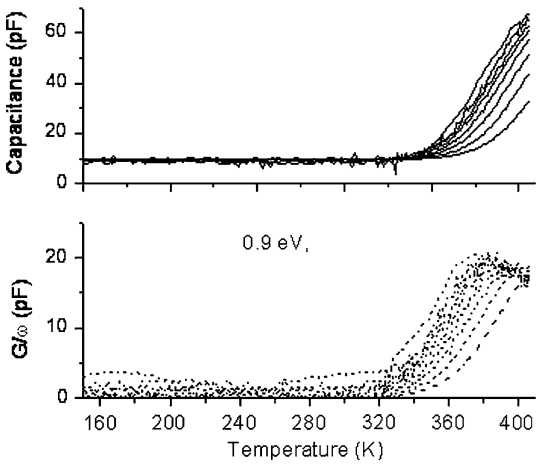

Fig. 3. Admittance spectra measured for the *n*-GaN ELOG sample irradiated with a dose of 2×10^{15} cm^{-2} neutrons; measurement frequencies 70, 100, 120, 150, 200, 300, 500, 1000 Hz. The curve for the lowest frequency is the one at the top in each case, and the highest frequency curve is at the bottom.

Deep Electron and Hole Traps from DLTS, ODLTS, PICTS

The evolution of DLTS spectra with neutron irradiation of ELOG samples is shown in Fig. 4. In the virgin sample electron traps with activation energies of 0.18, 0.25, 0.8, and 1 eV were observed. The concentrations of these traps, determined by the assumption that the shallow donor concentration was the one corresponding to a reverse bias of –2 V (10^{15} cm^{-3}), were, respectively, 10^{13}, 3×10^{13}, 3×10^{13}, and 10^{13} cm^{-3}, in agreement with earlier reported values for similarly grown ELOG samples.[20,21] Irradiation increased the concentrations of the 0.8 eV and 1 eV electron traps, while, for shallow traps, the changes were only slight (the decrease of the signal for the 0.18 eV and 0.25 eV traps for the dose of 10^{15} cm^{-2} is due to freeze-out of the sample capacitance at low temperatures). For higher doses, the Fermi level was pinned at deep centers near E_c –(0.8–0.9) eV and DLTS measurements were no longer possible. The 0.8 eV traps observed in DLTS and the 0.8–0.9 eV traps detected in admittance spectra of heavily irradiated samples are most likely the same centers.

The variation of hole trap spectra with neutron dose is shown in Fig. 5. The dominant hole traps in the virgin samples were the well-known E_v +0.9 eV hole traps commonly observed in undoped *n*-GaN films.[23,24] The signal from these traps decreased with neutron dose, because of the decreasing lifetime of minority carriers. A broad hole-trap feature, absent in the virgin sample, emerged after

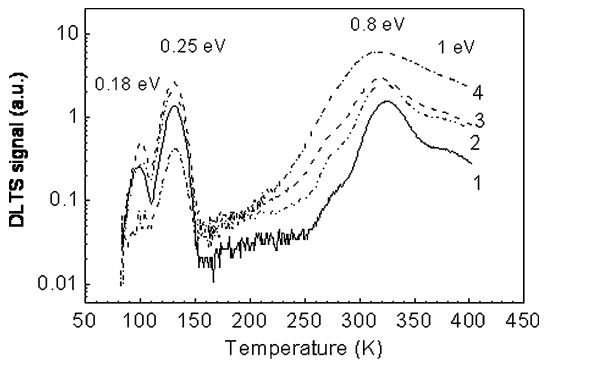

Fig. 4. DLTS spectra measured on *n*-GaN ELOG samples before irradiation (curve 1) and after irradiation with 4×10^{13} cm^{-2} (curve 2), 9×10^{13} cm^{-2} (curve 3), 10^{15} cm^{-2} (curve 4) neutrons.

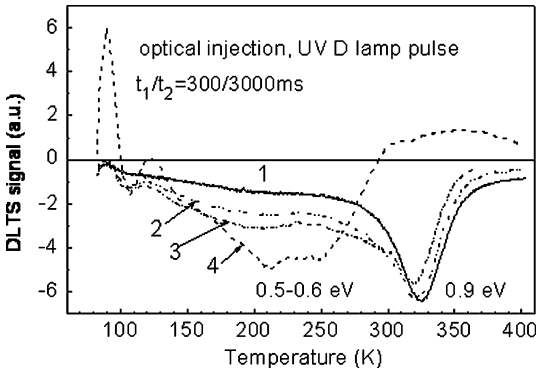

Fig. 5. DLTS spectra measured with D UV lamp optical injection measured on *n*-GaN ELOG samples before irradiation (curve 1) and after irradiation with 4×10^{13} cm^{-2}(curve 2), 9×10^{13} cm^{-2} (curve 3), 10^{15} cm^{-2} (curve 4).

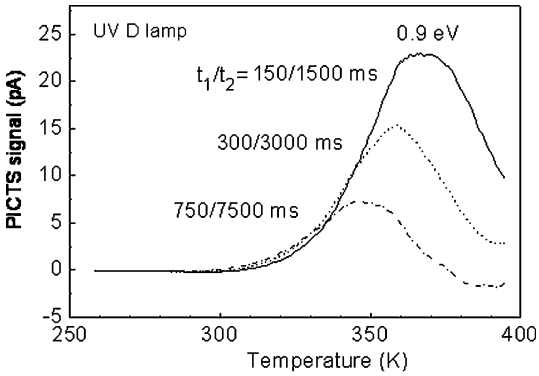

Fig. 7. PICTS spectra from *n*-GaN ELOG sample irradiated with 1.7×10^{17} cm^{-2} neutrons; measurements on a Au Schottky diode, at reverse bias of −10 V, with 5-s-long D UV lamp optical injection pulse; the spectra are shown for three time windows marked near the curves.

irradiation at temperatures between 150 K and 270 K (the low temperature hole-trap features in the figure come from interference with intense electron trap peaks). The activation energy for the peak position of this broad feature was 0.5–0.6 eV. However, comparison with ODLTS spectra obtained using optical injection pulses of GaAs IR light emitting diode array (Fig. 6) shows that the peak cannot be due to a true hole trap. Indeed, the photon energy for such IR excitation is 1.4 eV and cannot excite carriers from a center located much below the middle of the gap. The situation is similar to the one we observed in neutron irradiated undoped *n*-GaN films grown by MOCVD.[10] The emergence of the hole-trap feature near 0.6 eV in the ODLTS spectra of irradiated samples correlated very closely with an increase in the persistent photocapacitance (PPC) signal. The peak is due to excitation of electrons from a potential well formed by disordered regions in neutron irradiated GaN.[26] The return of excited carriers is associated with the overcoming of a high potential barrier which gives rise to both strong PPC effect and a hole-traps-like signal in ODLTS spectra. It is likely that the same disordered regions are responsible for the effect in our ELOG samples.

From the temperature dependence of conductivity in heavily irradiated (doses of 2×10^{17} cm^{-2}) and 10^{18} cm^{-2}) ELOG samples in which the disordered regions overlap, we can conclude that the Fermi level position in the DR core should be close to 0.95 eV.[11] Although the standard DLTS technique was not applicable to the samples heavily compensated with radiation, PICTS measurements[27] could still be performed. Figure 7 shows PICTS spectra taken on the sample irradiated with 2×10^{17} cm^{-2} neutrons. One trap with an activation energy of 0.95 eV was observed and is related to the traps pinning the Fermi level.

EBIC Results

Figure 8 shows the EBIC line scans across the ELOG stripes in the virgin sample and in the samples irradiated with 10^{15} cm^{-2} and 2×10^{15} cm^{-2} neutrons. The results are for a probe electron beam

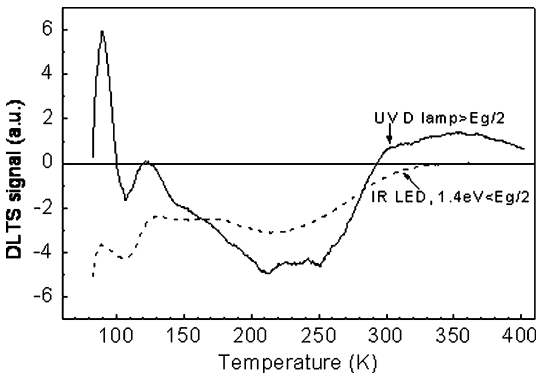

Fig. 6. DLTS spectra with optical injection measured for the *n*-GaN ELOG sample irradiated with a dose of 10^{15} cm^{-2} neutrons; the solid line depicts D UV lamp excitation; the dashed line depicts excitation with sub-bandgap radiation of GaAs light emitting diode array.

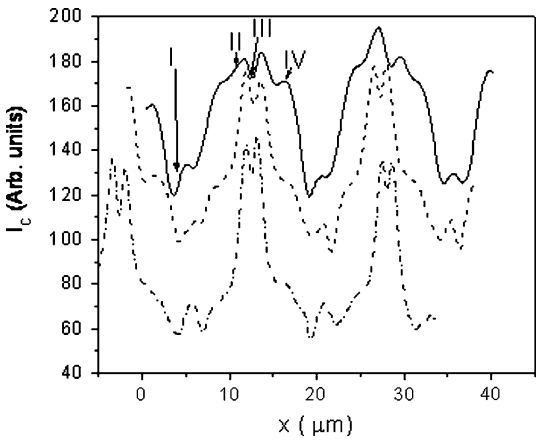

Fig. 8. EBIC signal I_c profiles taken across the *n*-GaN ELOG sample before irradiation (solid line) and after irradiation with 10^{15} cm^{-2} neutrons (dashed line) and 2×10^{15} cm^{-2} neutrons (dash-dotted line).

accelerating voltage of 22 kV. Three distinct regions are seen and are marked as regions I, II, III. Region I corresponds to the material grown in the windows of the SiO_2 mask with a high dislocation density of $(3–5) \times 10^8$ cm^{-2}. This region is characterized by a low collection efficiency of the EBIC signal. The second region is the area of the sample grown laterally over the SiO_2 mask with lower dislocation density of $\sim 5 \times 10^6$ cm^{-2}. Region III is in the middle of the SiO_2 stripes, where the two laterally overgrown areas propagating from the opposite ends of the window in the mask meet. Since the processes of lateral overgrowth on the opposite sides of the window are not correlated, the two ELOG regions are slightly misaligned and the misalignment is accommodated by the formation of a high density of dislocations ($\sim 10^8$ cm^{-2} in region III).[21] This region has a lowered EBIC signal. We also define one more region, region IV, located within the low-dislocation-density ELOG region II, but closer to the boundary with the high-dislocation-density region I. From the inspection of the other EBIC profiles corresponding to irradiated material, the signal in region IV decreases more rapidly than for region I. The EBIC signal collection efficiency in each region is determined by the local diffusion length of the charge carriers L_d and local concentration of the charged centers N_{SCR}. Measurements of the EBIC collection efficiency as a function of the accelerating beam voltage allows us to derive the local values of L_d and N_{SCR} by approximating the experimental curve with the model, curve using N_{SCR} and L_d as fitting parameters.[17–19] Calculations performed for the virgin sample gave, for regions I and II, the values of $N_{SCR} = 3 \times 10^{15}$ cm^{-3}, L_d = 0.17 μm (region I) and $N_{SRC} = 1 \times 10^{15}$ cm^{-3}, L_d = 0.3 μm (region II).[22] The results for region IV were the same as for region I.

After irradiation with 10^{15} cm^{-2} and 2×10^{15} cm^{-2} neutrons, the main effect is a stronger decrease of the EBIC signal in region IV than in region II, *i.e.*, the signal decreases much more strongly at the wings of the ELOG region. In EBIC images of the structures the low dislocation density ELOG area looks like a bright stripe.[20] The effect of radiation is to make these bright stripes look narrower than those in the virgin sample. From the dependence of the EBIC signal on the beam voltage, L_d and N_{SCR} in the irradiated samples were estimated. The diffusion length hardly changed at all for the dark region I for the doses 10^{15} cm^{-2} and 2×10^{15} cm^{-2}. For the laterally overgrown regions II and IV it decreased to the same value (0.17–0.19) μm after doses of $1–2 \times 10^{15}$ cm^{-2}.

For the density of the charged centers determining the width of the SCR, the main effect was the difference in N_{SCR} values in the ELOG proper area II and in the ELOG wings area IV, as illustrated by Fig. 9. For the first region, the N_{SCR} value increased slightly to 2×10^{15} cm^{-3} for the dose of 10^{15} cm^{-2} and hardly changed after the dose of 2×10^{15} cm^{-2}.

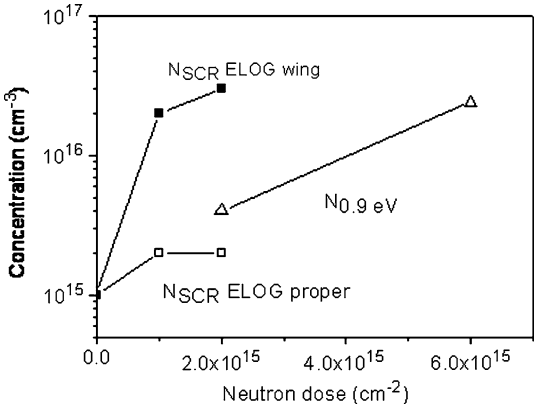

Fig. 9. Concentration of charged centers N_{SCR} deduced from the EBIC signal collection efficiency versus voltage dependancies; the results of the fitting versus neutron dose are shown for the laterally overgrown regions I (ELOG proper) and IV (ELOG wing); also shown is the dose dependence of the concentration of the 0.9 eV ($N_{0.9}$) electron trap calculated from low frequency *C–V* measurements at 400 K.

By contrast, for the ELOG wings region IV, the concentration increased steeply to 2×10^{16} cm^{-3} after 10^{15} cm^{-2} and to 3×10^{16} cm^{-3} for 2×10^{15} cm^{-2}. In ordinary *n*-type material, N_{SCR} is the concentration of uncompensated shallow donors. However, in compensated material, it is determined by the density of uncompensated deep centers at which the Fermi level is pinned outside the space charge region.[25] The obvious increase of the density of charged centers comes from the increase in the concentration of deep radiation defects that pin the Fermi level in the near-surface region. These defects are most likely the 0.8–0.9 eV electron traps observed in the low-frequency admittance spectra of the irradiated samples. In Fig. 9 we show the dependence of this concentration alongside N_{SCR}. Since the variations in local compensation ratio are not only dependent on the position across the sample but also on depth, the quantitative analysis of the EBIC dependence on the beam voltage and of the low frequency *C–V* characteristics is not accurate, but, qualitatively, the behavior looks similar.

DISCUSSION AND CONCLUSIONS

The results show that the main effects of neutron irradiation of ELOG *n*-GaN samples are the carrier removal and the introduction of deep electron traps with activation energies of 0.8 eV and 1 eV. There are also quasi-hole-trap defects, giving rise to a strong signal in DLTS spectra with optical excitation. After irradiation with doses $>10^{17}$ cm^{-2}, the samples become the heavily compensated *n*-type, with the Fermi level pinned near E_c –0.95 eV. These effects are similar to the ones observed for neutron irradiation of undoped *n*-GaN produced by standard MOCVD.[10,11] As in standard MOCVD GaN, the main contribution to the carrier removal rate in ELOG samples comes from disordered regions that

are also responsible for the quasi-hole-trap features in ODLTS of irradiated samples.[10,26] The Fermi level pinning position in heavily irradiated ELOG samples comes from the overlapping of the disordered regions and characterizes the position of the Fermi level in the core of these regions. The main contribution to the pinning of the Fermi level comes from electron traps with levels near 0.85 eV and 1 eV.

All these features are common to both ELOG and MOCVD films. The difference is in the five-times lower carrier removal rates and the several-times lower deep trap introduction rates averaged over the large area of the ELOG films compared to MOCVD layers. Quantitative deconvolution of these values into separate contributions of the low-dislocation density laterally overgrown region II and the high-dislocation-density SiO_2-mask-window region I is difficult, because of both lateral and depth non-uniformity of doping. The main contribution to the signal in *C–V* profiling of ELOG samples comes from the laterally overgrown regions; the donor concentration gradually increases with the distance from the surface, and the net doping in the laterally overgrown regions of the virgin sample is about three-times lower than in the high-dislocation-density window regions. The radiation damage spreads into the laterally overgrown regions from the boundary with the high-dislocation-density window region, confirmed by the large difference in the EBIC collection efficiency in regions II and IV of neutron irradiated samples and by the large difference in the introduction rates of the charged centers. The reason for the higher defect introduction rate in the ELOG wing region IV than in the ELOG proper region II is not clear. X-ray measurements of the lattice parameter changes in heavily neutron irradiated *n*-GaN MOCVD and ELOG films showed that the lattice parameter increase is about four-times higher in the MOCVD material, suggesting a more efficient formation of defects of the Ga interstitial type.[11]

ACKNOWLEDGEMENTS

The work at the Institute of Rare Metals (IRM) was supported in part by a grant from the Russian Foundation for Basic Research (RFBR grant # 05-02-08015) and ICTS (grant # 3029). The work at the University of Florida (UF) was partially supported by NSF DMR-040010.

REFERENCES

1. S. Nakamura, *GaN and Related Materials II*, ed. S.J. Pearton (New York: Gordon and Breach Science Publishers, 1999), pp. 1–45.
2. M.S. Shur and M.A. Khan, *GaN and Related Materials II*, ed. S.J. Pearton (New York: Gordon and Breach Science Publishers, 1999), pp. 47–92.
3. C.A. Usui, H. Sunakawa, A. Sakai, and A.A. Yamaguchi, *Jpn. J. Appl. Phys.* 36, L899 (1997).
4. D.C. Look, D.C. Reynolds, J.W. Hemsky, J.R. Sizelove, R.L. Jones, and R.J. Molnar, *Phys. Rev. Lett.* 79, 2273 (1997).
5. Z.-Q. Fang, D.C. Look, W. Kim, Z. Fan, A. Botchkarev, and H. Morkoc, *Appl. Phys. Lett.* 72, 2277 (1998).
6. S.A. Goodman, F.D. Auret, F.K. Koschnick, J.-M. Spaeth, B. Baumont, and P. Gibart, *Mater. Sci. Eng., B* B71, 100 (2000).
7. M. Hayes, F.D. Auret, L. Wu, W.E. Meyer, J.M. Nel, and M.J. Legodi, *Physica B* 340–342, 421 (2003).
8. P. Hacke, T. Detchprom, K. Hiramatsu, and N. Sawaki, *Appl. Phys. Lett.* 63, 2676 (1993).
9. A.Y. Polyakov, A.S. Usikov, B. Theys, N.B. Smirnov, A.V. Govorkov, F. Jomard, N.M. Shmidt, and W.V. Lundin, *Solid-State Electron.* 44, 1971 (2000).
10. A.Y. Polyakov, N.B. Smirnov, A.V. Govorkov, A.V. Markov, S.J. Pearton, N.G. Kolin, D.I. Merkurisov, V.M. Boiko, C.-R. Lee, and I.-H. Lee, *J. Vac. Sci. Technol., B* 25, 436 (2007).
11. A.Y. Polyakov, N.B. Smirnov, A.V. Govorkov, A.V. Markov, N.G. Kolin, D.I. Merkurisov, V.M. Boiko, K.D. Shcherbatchev, V.T. Bublik, M.I. Voronova, I-H. Lee, and C.R. Lee, *J. Appl. Phys.* 100, 093715 (2006).
12. D.C. Look, Z.-Q. Fang, and B. Claffin, *J. Cryst. Growth* 281, 143 (2005).
13. F.D. Auret, W.E. Meyer, L. Wu, M. Hayes, M.J. Legodi, B. Beaumont, and P. Gibart, *Phys. Status Solidi A* 201, 2271 (2004).
14. A.Y. Polyakov, N.B. Smirnov, A.V. Govorkov, A.V. Markov, J.H. Baek, C.-R. Lee, I.-H. Lee, N.G. Kolin, I.D. Merkurisov, V.M. Boiko, and S.J. Pearton, *Abstracts of European Workshop on III-Nitride Semiconductor Materials*, Heraklion, Crete, Greece, September 2006 (Heraklion: Heraklion University, 2006), pp. 82–83.
15. C.J. Wu and D.B. Wittry, *J. Appl. Phys.* 49, 2827 (1978).
16. J.Y. Chi and H.C. Gatos, *J. Appl. Phys.* 50, 3433 (1979).
17. C. Frigeri, *Inst. Phys. Conf. Ser.* 87, 745 (1987).
18. E.B. Yakimov, *Solid State Phenomena* V. 78–79, ed. H. Tokamage and T. Sekiguchi (Zuerich-Uetikon, Switzerland: Scitec Publications, 2001), pp. 79–85.
19. E.B. Yakimov, S.S. Borisov, and S.I. Zaitsev, *Russ. Phys. Semicond.* 41, 426 (2007).
20. I.-H. Lee, A.Y. Polyakov, N.B. Smirnov, A.V. Govorkov, A.V. Markov, and S.J. Pearton, *Phys. Status Solidi C* 3, 2087 (2006).
21. I.-H. Lee, A.Y. Polyakov, N.B. Smirnov, A.V. Govorkov, A.V. Markov, and S.J. Pearton, *Thin Solid Films*, 2007, in press.
22. E.B. Yakimov, P.S. Vergeles, A.Y. Polyakov, N.B. Smirnov, A.V. Govorkov, I.-H. Lee, C.-R. Lee, and S.J. Pearton, *Appl. Phys. Lett.* 90, 152114 (2007).
23. A.Y. Polyakov, N.B. Smirnov, A.V. Govorkov, M. Shin, M. Skowronski, and D.W. Greve, *J. Appl. Phys.* 84, 870 (1998).
24. A.Y. Polyakov, N.B. Smirnov, A.S. Usikov, A.V. Govorkov, and B.V. Pushniy, *Solid State Electron.* 42, 1959 (1998).
25. L.S. Berman and A.A. Lebedev, *Capacitance Spectroscopy of Deep Defects in Semiconductors* (Leningrad: Nauka, 1981)[in Russian].
26. B.R. Gossick, *J. Appl. Phys.* 30, 1214 (1959).
27. A.Y. Polyakov, N.B. Smirnov, A.V. Govorkov, and J.M. Redwing, *Solid State Electron.* 42, 831 (1998).